

Microscopic theory of multiterminal hybrid structures: self consistent superconducting order parameter, local density of states and point contact experiments

H. Jirari, R. Mélin and N. Stefanakis

Centre de Recherches sur les Très basses températures (CRTBT)
BP 166X, 38042 Grenoble Cedex, France*

We consider a microscopic theory of point contact experiments in multiterminal ferromagnet / superconductor hybrid structures in which three electrodes are connected to a superconductor. We suppose that the distance between the electrodes is smaller than the superconducting coherence length. We calculate the superconducting order parameter, the local density of state (LDOS) and transport properties. We show that the proximity effect in one of the electrodes can be controlled by the spin orientation of the other ferromagnetic electrodes in the sense that the LDOS in one of the electrodes depends strongly on the spin orientation of the other electrodes. With two ferromagnetic electrodes connected to a superconductor we find that the superconducting order parameter in the ferromagnetic alignment is larger than the superconducting order parameter in the antiferromagnetic alignment ($\Delta_F > \Delta_{AF}$) in agreement with [Eur. Phys. J. B **25**, 373 (2002)]. If a third spin polarized electrode is connected to a superconductor we find that $\Delta_F - \Delta_{AF}$ can change sign as the transparency of the third electrode increases. We calculate transport properties and provide a detailed discussion of averaging the phase of the ordinary and anomalous propagators for arbitrary interface transparencies.

I. INTRODUCTION

The manipulation of entangled states of electrons in condensed matter devices has focussed an important interest recently. The ground state of a superconductor is a condensate of Cooper pairs that form singlet states. Entangled states of electrons can thus be manipulated in transport experiments by extracting Cooper pairs out of a superconductor. Several experiments using a superconductor as a source of entangled states of electrons have been proposed recently. For instance it was shown in Ref. [1] that entangled states of electrons can be manipulated in a double dot experiment. A quantum teleportation experiment using three quantum dots has been proposed recently [2]. Another possible experiment has also been proposed in Ref. [3] in which a “beam splitter” is connected to a superconductor. In this situation noise correlations can reveal information about electronic entanglement [3]. Other experiments in which several ferromagnetic electrodes are connected to a superconductor have been investigated theoretically in Refs. [4–8].

There is a rich physics occurring at a single ferromagnet / superconductor (FS) interface. For instance Andreev reflection is suppressed if the spin polarization of the ferromagnetic metal increases. This is because the incoming electron and the reflected hole belong to different spin bands. As a consequence Andreev reflection can occur only in the channels having both a spin-up and a spin-down Fermi surface [9]. This theoretical prediction was well verified in experiments [10,11] and it was shown that with high transparency interfaces the suppression of Andreev reflection by spin polarization can be used to probe the Fermi surface polarization [10]. The results of the Andreev reflection experiments compare well with another method based on spin polarized tunneling in the presence of Zeeman splitting [12]. Another phenomenon taking place at FS interfaces is that the pair amplitude induced in a ferromagnetic metal can oscillate in space. This gives the possibility of fabricating π junctions in which the Josephson relation changes sign [13–19]. It is also well established that FS multilayers present oscillations of the superconducting critical temperature as the thickness of the ferromagnetic layer is varied [20–25]. Other new phenomena related to the proximity effect have also been investigated in diffusive FS heterostructures [26–31].

Multiterminal hybrid structures consist of systems in which several spin polarized electrodes are connected to a superconductor and are controlled by crossed Andreev reflection processes in which the spin-up and spin-down electrons making the Cooper pair can tunnel in different ferromagnetic electrodes. Several theoretical predictions have been made. For instance the current circulating in one of the electrodes can be controlled by the voltage applied on another electrode [5,7]. The conductance can be described in terms of a conductance matrix [5] that can be calculated from Keldysh formalism [7]. Other predictions concern the proximity effect in FSF trilayers [32]. It was shown in Ref. [8] that the two ferromagnetic electrodes of the FSF trilayer are coupled by pair correlations and that the

*U.P.R. 5001 du CNRS, Laboratoire conventionné avec l’Université Joseph Fourier

superconducting order parameter in the ferromagnetic alignment is larger than the superconducting order parameter in the antiferromagnetic alignment ($\Delta_F > \Delta_{AF}$). The formation of pair correlations among the two ferromagnets with metallic electrodes can be contrasted with the case of insulating ferromagnets where the superconducting order parameter is larger if the two ferromagnetic electrodes have an antiferromagnetic spin orientation ($\Delta_F > \Delta_{AF}$) because of pair breaking [33–35]. Because of the advances in nano-technology one may think that the proximity effect experiments with metallic ferromagnets will become possible in the future. The difficulty is to connect two ferromagnetic electrodes at a distance smaller than the superconducting coherence length.

We consider in this article possible experiments in which three metallic electrodes are connected to a superconductor at a distance smaller than the superconducting coherence length. One of the situations is shown on Fig. 1. In this point

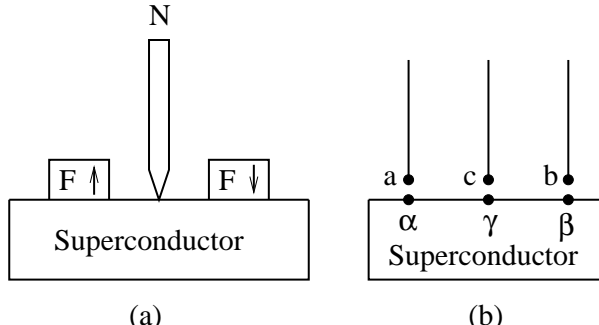


FIG. 1. (a): Schematic representation of the point contact experiments; (b): Representation of the model in which three electrodes are connected to a superconductor. A voltage V is applied on electrode c and the potentials of electrodes a and b are equal to the potential of the superconductor. There is thus no current flow through electrodes a and b .

contact experiment a normal metal electrode c is connected to a superconductor in the vicinity of two ferromagnetic electrodes a and b . The superconducting order parameter at point γ depends on the relative spin orientation of the ferromagnetic electrodes a and b . As a consequence the current through electrode c depends on the relative spin orientation of the ferromagnetic electrodes a and b . Measuring the current through electrode c is thus a local probe of the superconducting order parameter. In the situation on Fig. 1 the contact with the normal metal electrode can be a tunnel interface but we consider also a point contact situation. If the contact with electrode c has a large transparency pair correlations can be formed not only between the two ferromagnetic electrodes a and b but also between the ferromagnetic electrodes and the normal metal electrode c . If electrode c is ferromagnetic we find a change of sign in $\Delta_F - \Delta_{AF}$ as the transparency of the interface with electrode c is increased.

From the point of view of the method we use two complementary approaches: (i) an analytical estimation of the high energy behavior of the Gorkov function; (ii) exact diagonalizations of the Bogoliubov-de Gennes equations. In the analytical calculation we suppose that the band-width of the superconductor is much larger than the superconducting gap. As a consequence the integral in the self-consistency relation is dominated by the high-energy behavior. In the numerical simulation the band-width of the superconductor is not small compared to the superconducting gap (typically the ratio between the bandwidth and the gap is $\Delta/D \simeq 1/5$). The analytical calculation and the numerical simulation correspond to different regimes and this is why all the analytical results cannot be confirmed by the numerical simulation. The numerical simulation is useful to discuss the behavior of the local density of states (LDOS), the case of a partial spin polarization and the spatial variation of the pair amplitude.

The article is organized as follows. Technical preliminaries are given in section II. Section III is devoted to the case of a single FS interface. Using exact diagonalizations of the Bogoliubov-de Gennes Hamiltonian we find Andreev bound states that have been discussed recently by means of a recursion method [36]. In section IV we discuss the proximity effect in FSF heterostructures and generalize the results obtained in Ref. [8]. Namely we show that the superconducting order parameter is larger if the ferromagnetic electrodes have a parallel spin orientation. Multiterminal structures in which three electrodes are connected to a superconductor are discussed in section V. Transport properties are discussed in section VI. Concluding remarks are given in section VII.

II. PRELIMINARIES

We want to describe a situation where three spin polarized ferromagnetic electrodes are connected to a superconductor. We use two complementary approaches:

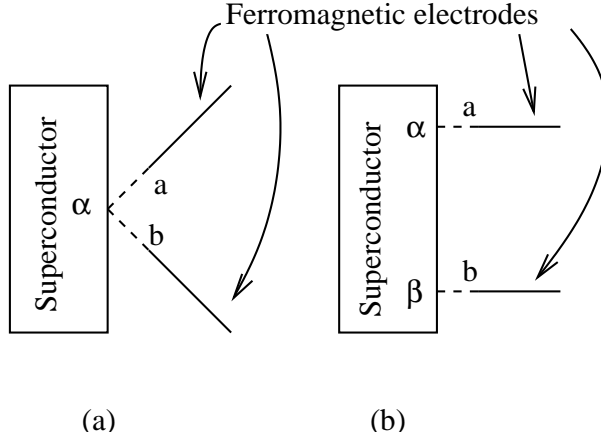


FIG. 2. The two models considered in sections IV A and IV B. In (a) the two ferromagnetic electrodes are connected to the same site in the superconductor. In (b) the two ferromagnetic electrodes are connected to two different sites in the superconductor. The two ferromagnetic electrodes contain a spin-up and a spin-down conduction band. The models are thus solved in a 4×4 formalism.

- (i) An analytical method based on Green's function formalism. With this method we evaluate the high energy behavior of the Gorkov function and deduce the self-consistent superconducting order parameter. We calculate also transport properties for arbitrary interface transparencies using Keldysh formalism. The technical details are given in section II A.
- (ii) A numerical method based on exact diagonalizations of the Bogoliubov-de Gennes Hamiltonian. With this method we calculate the superconducting order parameter, the pair amplitude and the LDOS. The technical details are given in section II B.

A. Green's function formalism

1. The models

The superconductor is described by a BCS lattice model

$$\mathcal{H}_{\text{BCS}} = \sum_{\langle\alpha,\beta\rangle,\sigma} -t (c_{\alpha,\sigma}^+ c_{\beta,\sigma} + c_{\beta,\sigma}^+ c_{\alpha,\sigma}) + \sum_{\alpha} (\Delta_{\alpha} c_{\alpha,\uparrow}^+ c_{\alpha,\downarrow} + \Delta_{\alpha}^* c_{\alpha,\downarrow} c_{\alpha,\uparrow}),$$

where Δ_{α} is the pairing interaction. The brackets indicate that hopping is between nearest neighbors. The ferromagnetic electrodes are described by a lattice Stoner model

$$\mathcal{H}_{\text{Stoner}} = \sum_{\langle i,j \rangle,\sigma} -t (c_{i,\sigma}^+ c_{j,\sigma} + c_{j,\sigma}^+ c_{i,\sigma}) - h \sum_i (c_{i,\uparrow}^+ c_{i,\uparrow} - c_{i,\downarrow}^+ c_{i,\downarrow}),$$

where h is the exchange field. An exchange field smaller than the bandwidth corresponds to a partially polarized ferromagnet and an exchange field larger than the bandwidth corresponds to a half-metal ferromagnet in which only majority spins are present. We note ρ_0^S the density of states in the superconductor and ρ_{σ}^F the spin- σ density of states in the ferromagnetic electrodes. We use Greek symbols α, β, γ for the sites in the superconductor and Latin symbols a, b, c for the sites in the ferromagnetic electrodes. The tunnel Hamiltonian coupling the superconductor and the ferromagnetic electrodes takes the form

$$\hat{\mathcal{W}} = \sum_{k,\sigma} t_{a_k,\alpha_k} (c_{a_k,\sigma}^+ c_{\alpha_k,\sigma} + c_{\alpha_k,\sigma}^+ c_{a_k,\sigma}), \quad (1)$$

where the sum over k runs over all contacts between the superconductor and the ferromagnetic electrodes.

2. Green's functions

The Green's functions of a connected system are obtained by solving the Dyson equation in the Nambu representation:

$$\hat{G}^{R,A} = \hat{g}^{R,A} + \hat{g}^{R,A} \otimes \hat{\Sigma} \otimes \hat{G}^{R,A}, \quad (2)$$

where the self-energy $\hat{\Sigma}$ contains all couplings of the tunnel Hamiltonian given by (1). The Green's functions g correspond to the “disconnected” system in which $t_{a_k, \alpha_k} = 0$ (see Eq. 1). The Dyson equation (2) is used to calculate the Green's functions of the connected system in which an electron in the superconductor can make excursions in the ferromagnetic electrodes.

We use the following notation for the Nambu representation of the advanced and retarded propagators of the disconnected system:

$$\hat{g}^{A,R}(t, t') = \begin{pmatrix} g^{A,R}(t, t') & f^{A,R}(t, t') \\ f^{A,R}(t, t') & g^{A,R}(t, t') \end{pmatrix},$$

with

$$g^A(t, t') = -i\theta(t - t') \langle \{c_{i,\uparrow}(t), c_{j,\uparrow}^\dagger(t')\} \rangle \quad (3)$$

$$f^A(t, t') = -i\theta(t - t') \langle \{c_{i,\uparrow}(t), c_{j,\downarrow}(t')\} \rangle, \quad (4)$$

and we use the following notation for the Nambu representation of the density of states:

$$\hat{\rho} = \begin{pmatrix} \rho_g & \rho_f \\ \rho_f & \rho_g \end{pmatrix},$$

with $\rho_g = \frac{1}{\pi} \text{Im}(g^A)$ and $\rho_f = \frac{1}{\pi} \text{Im}(f^A)$. The Keldysh Green's function is obtained through the Dyson-Keldysh equation

$$\hat{G}^{+,-} = [\hat{I} + \hat{G}^R \otimes \hat{\Sigma}] \otimes \hat{g}^{+,-} \otimes [\hat{I} + \hat{\Sigma} \otimes \hat{G}^A], \quad (5)$$

where $\hat{g}_{i,j}^{+,-} = 2i\pi n_F(\omega - \mu_{i,j})\hat{\rho}_{i,j}$.

3. Superconducting order parameter and transport properties

In equilibrium the Keldysh Green's function defined by Eq. (5) simplifies into

$$\hat{G}_{\text{eq}}^{+,-} = n_F(\omega - \mu_0) (\hat{G}^A - \hat{G}^R), \quad (6)$$

where μ_0 is the chemical potential, identical in all conductors. The form (6) of the Keldysh Green's function at equilibrium can be used to obtain the superconducting order parameter in the superconductor via the self-consistency equation

$$\Delta_\beta = -U \int \frac{d\omega}{2i\pi} G_{\beta,\beta}^{+,-,1,2}(\omega).$$

The Keldysh Green's function can also be used to obtain the current:

$$I_{a_k, \alpha_k} = \frac{e}{h} \int \text{Tr} \left\{ \hat{\sigma}^z \left[\hat{t}_{a_k, \alpha_k} \hat{G}_{\alpha_k, a_k}^{+,-} - \hat{t}_{\alpha_k, a_k} \hat{G}_{a_k, \alpha_k}^{+,-} \right] \right\} d\omega.$$

4. Green's functions of an isolated superconductor

The Green's function of the isolated superconductor with a uniform superconducting order parameter Δ_0 is obtained by evaluating the spectral representation [7]:

$$\hat{g}_{\alpha,\beta} = \pi \rho_0^S \frac{a_0}{R_{\alpha,\beta}} \exp \left[-\frac{R_{\alpha,\beta}}{2\xi(\omega)} \right] \left\{ \frac{\sin \varphi_{\alpha,\beta}}{\sqrt{\Delta_0^2 - \omega^2}} \begin{bmatrix} -\omega & \Delta_0 \\ \Delta_0 & -\omega \end{bmatrix} - \cos \varphi_{\alpha,\beta} \begin{bmatrix} 1 & 0 \\ 0 & 1 \end{bmatrix} \right\}. \quad (7)$$

Above the superconducting gap the Green's function (7) becomes $\hat{g}_{\alpha,\beta} = i\pi\hat{\rho}_{\alpha,\beta}$, where the density of states $\hat{\rho}_{\alpha,\beta}$ is given by

$$\hat{\rho}_{\alpha,\beta} = \rho_0^S \frac{a_0}{R_{\alpha,\beta}} \left\{ \frac{-\sin \varphi_{\alpha,\beta}}{\sqrt{\omega^2 - \Delta_0^2}} \begin{bmatrix} -\omega & \Delta_0 \\ \Delta_0 & -\omega \end{bmatrix} + i \cos \varphi_{\alpha,\beta} \begin{bmatrix} 1 & 0 \\ 0 & 1 \end{bmatrix} \right\}. \quad (8)$$

The phase variable in Eqs. 7 and 8 is $\varphi_{\alpha,\beta} = k_F R_{\alpha,\beta}$. The “local” propagators corresponding to $\alpha = \beta$ are described by $\varphi_{\alpha,\beta} = \pi/2$ [40]:

$$\hat{g}_{\text{loc}} = \pi \rho_0^S \frac{1}{\sqrt{\Delta_0^2 - \omega^2}} \begin{bmatrix} -\omega & \Delta_0 \\ \Delta_0 & -\omega \end{bmatrix} \quad (9)$$

$$\hat{\rho}_{\text{loc}} = \rho_0^S \frac{1}{\sqrt{\omega^2 - \Delta_0^2}} \begin{bmatrix} \omega & -\Delta_0 \\ -\Delta_0 & \omega \end{bmatrix} \quad (10)$$

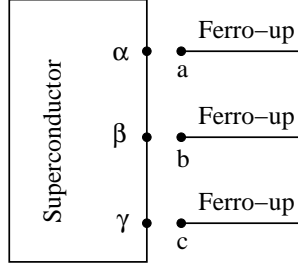


FIG. 3. Schematic representation of the model considered in section II A 5 in which three half-metal ferromagnet electrodes are connected to a superconductor.

5. Dyson matrix

In this section we provide a derivation of the Dyson matrix in the simple case of three half-metal ferromagnetic electrodes connected to a superconductor (see Fig. 3). If λ is an arbitrary site in the superconductor, the Dyson equation (2) becomes

$$\hat{G}^{a_n, \lambda} = \begin{bmatrix} K_{1,1}^{a_n, \lambda} & K_{1,2}^{a_n, \lambda} \\ -K_{2,1}^{a_n, \lambda} & -K_{2,2}^{a_n, \lambda} \end{bmatrix} + \sum_m \begin{bmatrix} K_{1,1}^{a_n, \alpha_m} & -K_{1,2}^{a_n, \alpha_m} \\ -K_{2,1}^{a_n, \alpha_m} & K_{2,2}^{a_n, \alpha_m} \end{bmatrix} t_{\alpha_m, a} \hat{G}^{a_m, \lambda}, \quad (11)$$

with $K_{i,j}^{a_n, \alpha_m} = g_{i,i}^{a_n, a_n} t_{a_n, \alpha_m} g_{i,j}^{\alpha_n, \alpha_m}$, and

$$\hat{G}^{a_n, \lambda} = \begin{bmatrix} G_{1,1}^{a_n, \lambda} & G_{1,2}^{a_n, \lambda} \\ G_{2,1}^{a_n, \lambda} & G_{2,2}^{a_n, \lambda} \end{bmatrix}. \quad (12)$$

Eqs. (11) and (12) are valid for an arbitrary spin polarization. In the case of the heterostructure on Fig. 3 the explicit form of the Dyson matrix is the following:

$$\begin{bmatrix} 1 - K_{1,1}^{a, \alpha} t_{\alpha, a} & -K_{1,1}^{a, \beta} t_{\beta, b} & -K_{1,1}^{a, \gamma} t_{\gamma, c} \\ -K_{1,1}^{b, \alpha} t_{\alpha, a} & 1 - K_{1,1}^{b, \beta} t_{\beta, b} & -K_{1,1}^{b, \gamma} t_{\gamma, c} \\ -K_{1,1}^{c, \alpha} t_{\alpha, a} & -K_{1,1}^{c, \beta} t_{\beta, b} & 1 - K_{1,1}^{c, \gamma} t_{\gamma, c} \end{bmatrix} \begin{bmatrix} G_{1,1}^{a, \lambda} \\ G_{1,1}^{b, \lambda} \\ G_{1,1}^{c, \lambda} \end{bmatrix} = \begin{bmatrix} K_{1,1}^{a, \lambda} \\ K_{1,1}^{b, \lambda} \\ K_{1,1}^{c, \lambda} \end{bmatrix}.$$

In sections III and IV and in the Appendices we invert a similar form of the Dyson matrix in models involving four channels.

B. Exact diagonalizations of the Bogoliubov-de Gennes Hamiltonian

In the numerical simulations based on exact diagonalizations of the Bogoliubov-de Gennes Hamiltonian we use a lattice Hubbard model

$$\mathcal{H} = \sum_{\langle\alpha,\beta\rangle,\sigma} -t (c_{\alpha,\sigma}^+ c_{\beta,\sigma} + c_{\beta,\sigma}^+ c_{\alpha,\sigma}) + \mu \sum_{\alpha,\sigma} n_{\alpha,\sigma} + \sum_{\alpha,\sigma} \mu_{\alpha}^I n_{\alpha,\sigma} + \sum_{\alpha,\sigma} h_{\alpha,\sigma} n_{\alpha,\sigma} + V_0 \sum_{\alpha} n_{\alpha,\uparrow} n_{\alpha,\downarrow}. \quad (13)$$

In Eq. (13) $n_{\alpha,\sigma} = c_{\alpha,\sigma}^+ c_{\alpha,\sigma}$ is the electron number operator at site α , μ is the chemical potential, $h_{\alpha,\sigma} = -h\sigma_z$ is the exchange field in the ferromagnetic region and $\sigma_z = \pm 1$ is the eigenvalue of the z component of the Pauli matrix. V_0 is the on-site interaction. We use negative values of V_0 corresponding to attractive interaction. To simulate the effect of depletion of the carrier density at the surface the site-dependent impurity potential μ_{α}^I is set to a sufficiently large value at the surface sites. This prohibits electron tunneling over these sites. Within a mean field approximation Eq. (13) reduces to the Bogoliubov-de Gennes equations [37,38]:

$$\begin{pmatrix} \hat{\xi} & \hat{\Delta} \\ \hat{\Delta}^* & -\hat{\xi} \end{pmatrix} \begin{pmatrix} u_{n,\uparrow}(r_{\alpha}) \\ v_{n,\downarrow}(r_{\alpha}) \end{pmatrix} = \epsilon_{n,\gamma_1} \begin{pmatrix} u_{n,\uparrow}(r_{\alpha}) \\ v_{n,\downarrow}(r_{\alpha}) \end{pmatrix}, \quad (14)$$

and

$$\begin{pmatrix} \hat{\xi} & \hat{\Delta} \\ \hat{\Delta}^* & -\hat{\xi} \end{pmatrix} \begin{pmatrix} u_{n,\downarrow}(r_{\alpha}) \\ v_{n,\uparrow}(r_{\alpha}) \end{pmatrix} = \epsilon_{n,\gamma_2} \begin{pmatrix} u_{n,\downarrow}(r_{\alpha}) \\ v_{n,\uparrow}(r_{\alpha}) \end{pmatrix}, \quad (15)$$

such that

$$\hat{\xi} u_{n,\sigma}(r_{\alpha}) = -t \sum_{\delta} u_{n,\sigma}(r_{\alpha} + \hat{\delta}) + (\mu^I(r_{\alpha}) + \mu) u_{n,\sigma}(r_{\alpha}) + h_{\alpha} \sigma_z u_{n,\sigma}(r_{\alpha}) \quad (16)$$

$$\hat{\Delta} u_{n,\sigma}(r_{\alpha}) = \Delta_0(r_{\alpha}) u_{n,\sigma}(r_{\alpha}), \quad (17)$$

and where the pair potential is defined by

$$\Delta_0(r_{\alpha}) = V_0 \langle c_{\uparrow}(r_{\alpha}) c_{\downarrow}(r_{\alpha}) \rangle.$$

In Eq. (16) $\hat{\delta} = \hat{x}, -\hat{x}, \hat{y}, -\hat{y}$ denotes the four directions of the square lattice. $\hat{\delta} = \hat{z}, -\hat{z}$ corresponds to the two directions in the ferromagnetic electrodes. The self-consistency equation takes the form

$$\Delta_0(r_{\alpha}) = \frac{V_0(r_{\alpha})}{2} F(r_{\alpha}) = \frac{V_0(r_{\alpha})}{2} \sum_n \left[u_{n,\uparrow}(r_{\alpha}) v_{n,\downarrow}^*(r_{\alpha}) \tanh \left(\frac{\beta \epsilon_{n,\gamma_1}}{2} \right) + u_{n,\downarrow}(r_{\alpha}) v_{n,\uparrow}^*(r_{\alpha}) \tanh \left(\frac{\beta \epsilon_{n,\gamma_2}}{2} \right) \right], \quad (18)$$

where β is the inverse temperature. We start from an approximate solution for the gap profile $\Delta_0(r_{\alpha})$. After exact diagonalizations of Eqs. (14) and (15) we obtain $u_{n,\sigma}(r_{\alpha})$ and $v_{n,\sigma}(r_{\alpha})$. The quasiparticle amplitudes are inserted into Eq. (18) and a new gap function is evaluated which is then inserted into Eq. (17) and we iterate until a sufficient precision has been obtained. Although the pair potential $\Delta_0(r_{\alpha})$ is zero in the ferromagnet the pair amplitude $F(r_{\alpha})$ is non zero. The LDOS at site α is given by

$$\rho_{\alpha}(E) = - \sum_{n,\sigma} [|u_{n,\sigma}(r_{\alpha})|^2 f'(E - \epsilon_n) + |v_{n,\sigma}(r_{\alpha})|^2 f'(E + \epsilon_n)], \quad (19)$$

where f' is the derivative of the Fermi function $f(\epsilon) = \frac{1}{1 + \exp(\epsilon/k_B T)}$.

III. PROXIMITY EFFECT AT A SINGLE FS INTERFACE

We first use exact diagonalizations of the Bogoliubov-de Gennes equations (see section II B) to describe the proximity effect at a single FS interface. This constitutes a test of our method and we recover some of the results for the LDOS obtained recently by means of a recursion method (see Ref. [36]).

We consider a two-dimensional superconducting system of 30×30 sites and we suppose fixed boundary conditions by setting the impurity potential $\mu^I = 100t$ at the surface. The temperature is $k_B T = 0.1t$ and the local attractive

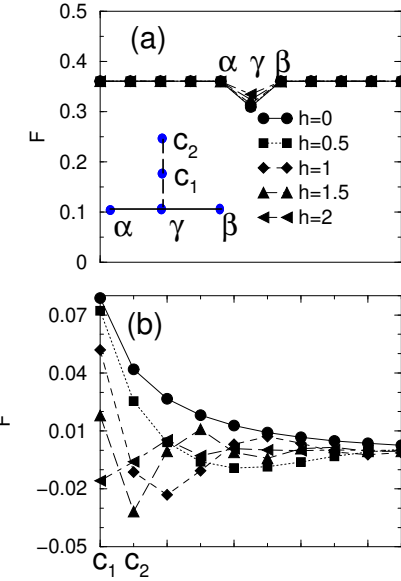


FIG. 4. (a) Pair amplitude for different values of the exchange field for several sites in the superconducting region at the interface of one-dimensional ferromagnetic electrode and a two-dimensional superconducting system. Sites α, γ, β belong to the superconductor while the sites c_1, c_2 belong to the ferromagnetic electrode. (b) Pair amplitude for several sites in the ferromagnetic region for different values of the exchange field. The pair amplitude in the superconductor does not vary much with the exchange field. The pair amplitude in the ferromagnetic electrode shows an oscillatory behavior. The pair amplitude decays monotonically in the absence of spin polarization in the ferromagnetic electrode.

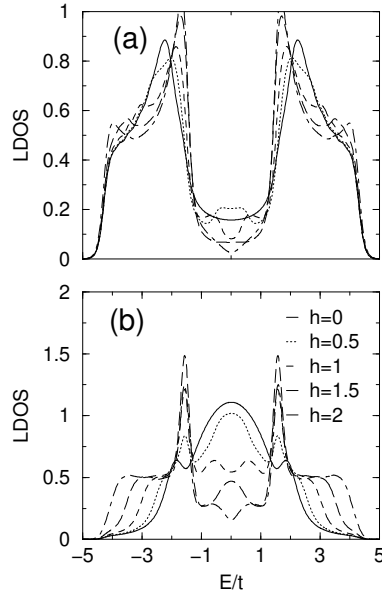


FIG. 5. (a) The LDOS at site γ in the superconductor for different values of the exchange field, for the geometry of Fig. 4. (b) The LDOS at site c_1 in the ferromagnetic electrode for different values of the exchange field. The subgap LDOS is due to Andreev bound states.

interaction in the superconducting region is $V_0 = -3.5t$. On top of the superconductor is attached a one-dimensional superconducting electrode of 50 sites. The transparency of the interface is controlled by changing the hopping element t_c connecting sites on both sides of the interface and we restrict here to the case where the transparency of the interface is the same as inside the superconductor. In this case the pair amplitude in the superconducting system is not really modified as seen in Fig. 4(a) while in the ferromagnetic region the pair amplitude oscillates around zero and the period of oscillations decreases with increasing the exchange field (see Fig. 4(b)). In the case of a zero exchange field the pair amplitude is decaying monotonically in the normal metal.

Due to the proximity effect the LDOS shows a gap structure even for the sites within the ferromagnet (see Fig. 5(b)). The conductance peaks within the gap are due to Andreev bound states [39] and have been discussed recently for a three dimensional FS interface using a recursion method [36]. The residual values of the LDOS are reduced by the increase of the exchange field. The Andreev bound states move towards the Fermi level and cross the Fermi level with increasing the exchange field.

IV. PROXIMITY EFFECT IN FSF HETEROSTRUCTURES

Now we reconsider the proximity effect in a FSF heterostructure in which two ferromagnetic electrodes are connected to a superconductor. It was shown in Ref. [8] that with metallic ferromagnets the superconducting order parameter in the ferromagnetic alignment is larger than in the antiferromagnetic alignment ($\Delta_F > \Delta_{AF}$). It was supposed in Ref. [8] that the two ferromagnetic electrodes are at a distance comparable to the superconducting coherence length and the Gorkov function was evaluated at a point in the superconductor far away from the contacts with the ferromagnetic electrodes. We discuss here two different situations (see Fig. 2):

- (i) A “local” model in which the distance between the contacts with the two ferromagnetic electrodes is smaller than the superconducting coherence length. In this situation the superconducting order parameter is uniform in space and we consider thus a simplified “local” model in which the two ferromagnetic electrodes are connected to the same site in the superconductor (see Fig. 2-(a)).
- (ii) A situation in which the distance between the contacts with the ferromagnetic electrodes is larger than the superconducting coherence length (see Fig. 2-(b)). In this situation we expand the Gorkov function in $1/R_{\alpha,\beta}$, where $R_{\alpha,\beta}$ is the separation between the ferromagnetic electrodes.

In both cases we obtain $\Delta_F > \Delta_{AF}$ which confirms the result obtained in Ref. [8].

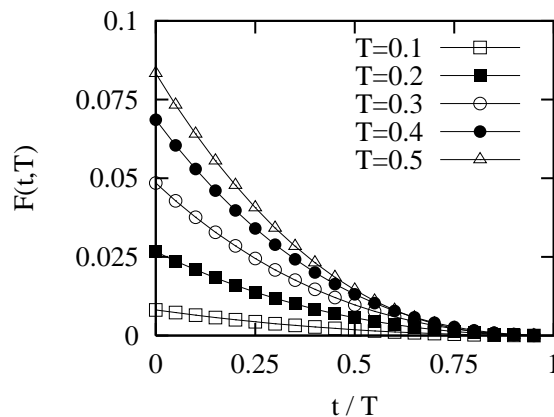


FIG. 6. Variation of $F(t, T)$ for different values of $T < 1/2$. We obtain $F(t, T) > 0$ which shows that the ferromagnetic superconducting order parameter is larger than the antiferromagnetic superconducting order parameter for large interface transparencies. The microscopic interaction U is such that the bulk superconducting gap is $\Delta_{\text{bulk}} = 1$ and the bandwidth of the superconductor is $D = 100$.

A. Two ferromagnetic electrodes at a distance smaller than the superconducting coherence length

1. Sign of $\Delta_F - \Delta_{AF}$

Let us start with the situation where the two ferromagnetic electrodes are at a distance smaller than the superconducting coherence length. In this case the spatial variation of the superconducting order parameter can be neglected and we thus consider a model in which the two electrodes are connected to the same site (see Fig. 2-(a)). We suppose that each ferromagnetic electrode is partially spin polarized and contains two spin channels. The model is thus solved in a 4×4 formalism. The Green's function $G_{\alpha,\alpha}^{A,1,2}$ is found to be

$$\begin{aligned} G_{\alpha,\alpha}^{A,1,2} = & -i\pi\rho_0^S \frac{\Delta}{\omega} - i\pi\rho_0^S \frac{\Delta}{\omega} \frac{1}{\mathcal{D}} \{ -f(x_{a,\uparrow}) - f(x_{a,\downarrow}) - f(x_{b,\uparrow}) - f(x_{b,\downarrow}) + 2f(x_{a,\uparrow})f(x_{b,\uparrow}) + 2f(x_{a,\downarrow})f(x_{b,\downarrow}) \\ & + f(x_{a,\uparrow})f(x_{a,\downarrow}) + f(x_{a,\uparrow})f(x_{b,\downarrow}) + f(x_{a,\downarrow})f(x_{b,\uparrow}) + f(x_{b,\uparrow})f(x_{b,\downarrow}) - f(x_{a,\uparrow})f(x_{a,\downarrow})f(x_{b,\downarrow}) \\ & - f(x_{a,\uparrow})f(x_{a,\downarrow})f(x_{b,\uparrow}) - f(x_{a,\downarrow})f(x_{b,\uparrow})f(x_{b,\downarrow}) - f(x_{a,\uparrow})f(x_{b,\uparrow})f(x_{b,\downarrow}) - f(x_{a,\uparrow})f(x_{a,\downarrow})f(x_{b,\downarrow}) \}, \end{aligned} \quad (20)$$

with

$$\mathcal{D} = (1 - f(x_{a,\downarrow})f(x_{b,\downarrow})) (1 - f(x_{a,\uparrow})f(x_{b,\uparrow})). \quad (21)$$

The interface transparencies are parametrized by $f(x_i) = x_i/(1+x_i)$, with $x_{a,\uparrow} = \pi^2 t_{a,\alpha}^2 \rho_{a,\uparrow}^F \rho_0^S$, $x_{a,\downarrow} = \pi^2 t_{a,\alpha}^2 \rho_{a,\downarrow}^F \rho_0^S$, $x_{b,\uparrow} = \pi^2 t_{b,\beta}^2 \rho_{b,\uparrow}^F \rho_0^S$, $x_{b,\downarrow} = \pi^2 t_{b,\beta}^2 \rho_{b,\downarrow}^F \rho_0^S$. The values of $f(x_i)$ are such that $0 < f(x_i) < 1/2$. We do not consider the regime $1/2 < f(x_i) < 1$ for which the self-consistency relation becomes unstable.

We suppose that the two ferromagnets have an identical density of states and that the two contacts have identical transparencies. In the ferromagnetic alignment we use the notation $f(x_{a,\uparrow}) = f(x_{b,\uparrow}) = T$ and $f(x_{a,\downarrow}) = f(x_{b,\downarrow}) = t$. In the antiferromagnetic alignment we use the notation $f(x_{a,\uparrow}) = f(x_{b,\downarrow}) = T$ and $f(x_{a,\downarrow}) = f(x_{b,\uparrow}) = t$. To second order in T and t we obtain

$$G_{\alpha,\alpha}^{1,2,F} - G_{\alpha,\alpha}^{1,2,AF} = -i\pi\rho_0^S \frac{\Delta}{\omega} (T-t)^2. \quad (22)$$

As a consequence in the regime of small interfaces transparencies we obtain $\Delta_F > \Delta_{AF}$. The regime of a large interface transparencies can be treated by evaluating numerically the difference between the Gorkov functions $G_{\alpha,\alpha}^{1,2,F} - G_{\alpha,\alpha}^{1,2,AF} = -i\pi\rho_0^S \frac{\Delta}{\omega} F(T,t)$. It is visible on Fig. 6 that $F(T,t)$ is positive for any value of $T < 1/2$ and $t < T$ so that the ferromagnetic superconducting order parameter is larger than the antiferromagnetic superconducting order parameter, in agreement with Ref. [8].

B. Two ferromagnetic electrodes at a distance comparable to the superconducting coherence length

Now we consider the model on Fig. 2-(b) where the distance between the two ferromagnetic electrodes is comparable to the superconducting coherence length (see Appendix A). We suppose that the contacts with the two ferromagnets have the same transparency and we use the notation $f(x_{a,\uparrow}) = f(x_{b,\uparrow}) = T$, $f(x_{a,\downarrow}) = f(x_{b,\downarrow}) = t$ in the ferromagnetic alignment, and $f(x_{a,\uparrow}) = f(x_{b,\downarrow}) = T$, $f(x_{a,\downarrow}) = f(x_{b,\uparrow}) = t$ in the antiferromagnetic alignment. With these assumptions the superconducting order parameter at point α is equal to the superconducting order parameter at point β . We obtain

$$G_{\alpha,\alpha}^{1,2,F} - G_{\alpha,\alpha}^{1,2,AF} = G_{\beta,\beta}^{1,2,F} - G_{\beta,\beta}^{1,2,AF} = -i\pi\rho_0^S \frac{\Delta}{\omega} \left(\frac{a_0}{R_{\alpha,\beta}} \right)^2 (T-t)^2 (1-T)(1-t),$$

from what we deduce that the superconducting order parameter in the ferromagnetic alignment is larger than the superconducting order parameter in the antiferromagnetic alignment. This is in agreement with Ref. [8].

C. Local density of states

We calculated the LDOS for a partial spin polarization by means of exact diagonalizations of the Bogoliubov-de Gennes Hamiltonian. The Andreev bound states depend strongly on the relative spin orientation of the ferromagnetic electrodes. It is visible on Fig. 8 that for a strong exchange field the low energy density of states is larger in the antiferromagnetic alignment than in the ferromagnetic alignment. This can be interpreted in terms of non local pair

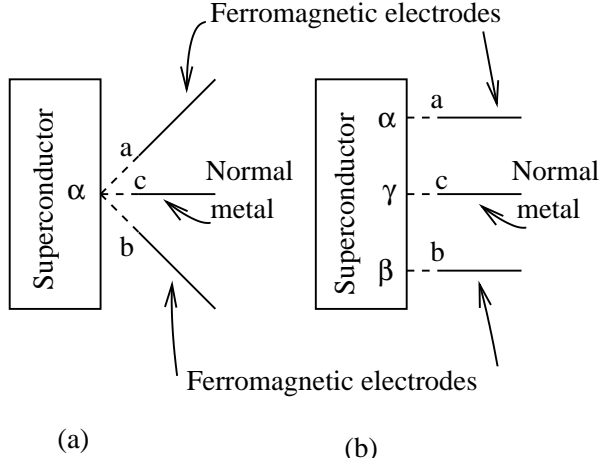


FIG. 7. The model considered in section V. In (a) the three electrodes are connected to the same site in the superconductor. In (b) the three electrodes are connected to two different sites in the superconductor. We use the model (a) to calculate the superconducting order parameter and we use the model (b) in section VI to calculate the transport properties.

correlations that are generated between the two ferromagnetic electrodes [8] due to crossed Andreev reflections as well as Andreev reflections within the same electrode. The weight of the low energy degrees of freedom is larger in the antiferromagnetic alignment because the antiferromagnetic spin configuration is compatible with the formation of superconducting correlations among the two ferromagnets due to crossed Andreev reflections. This is illustrated on Fig. 9 where we have represented the variation of the zero energy density of states as a function of the exchange field for the two spin orientations of the ferromagnetic electrodes.

V. PROXIMITY EFFECT IN MULTITERMINAL HYBRID STRUCTURES

In this section we consider an heterostructure in which three electrodes are connected to a superconductor at a distance smaller than the superconducting coherence length. With this assumption the superconducting order parameter can be considered as uniform in space. Similarly to section IV we use a “local” model in which the three electrodes are connected to the same site. We consider only the case where the distance between the electrodes is small compared to the superconducting coherence length. Electrodes a and b on Fig. 7 will be considered to be half-metal ferromagnets so that the models are solved in a 4×4 formalism. Using partially polarized ferromagnets would require to solve a 6×6 formalism for which we could not carry out the analytical calculation. The case of partially polarized ferromagnets will be treated numerically within exact diagonalizations of the Bogoliubov de Gennes equations.

A. Three electrodes at a distance smaller than the superconducting coherence length

We consider a model in which three electrodes are connected to the same site α (see Fig. 7-(a)). We determine the variation of $\Delta_F - \Delta_{AF}$ as a function of the transparency t_c of the contact with electrode c . We show that there is no change in the sign of $\Delta_F - \Delta_{AF}$ as t_c increases if electrode c is a normal metal. There is a change of sign in $\Delta_F - \Delta_{AF}$ as t_c increases if electrode c is a ferromagnet with a spin-down orientation.

B. Sign of $\Delta_F - \Delta_{AF}$

The expression of the Gorkov function in the ferromagnetic and antiferromagnetic alignments are given in Appendices B 1 and B 2. The variation of $\Delta_{\alpha,\alpha}^F - \Delta_{\alpha,\alpha}^{AF}$ as a function of the transparency of the contact with electrode c is shown on Fig. 10. It is visible on this figure that $\Delta_F > \Delta_{AF}$ for all values of the transparency $f(x_c)$ with interface c .

We also evaluated $\Delta_F - \Delta_{AF}$ in the case where electrode c is a half-metal ferromagnet with a spin-down orientation. We obtain a change of sign in $\Delta_{\alpha,\alpha}^F - \Delta_{\alpha,\alpha}^{AF}$ as the transparency of the interface with the ferromagnetic electrode c is increased (see Fig. 11). This change of sign can be described by expanding the Gorkov functions to second order in $f(x_a)$ and $f(x_b)$:

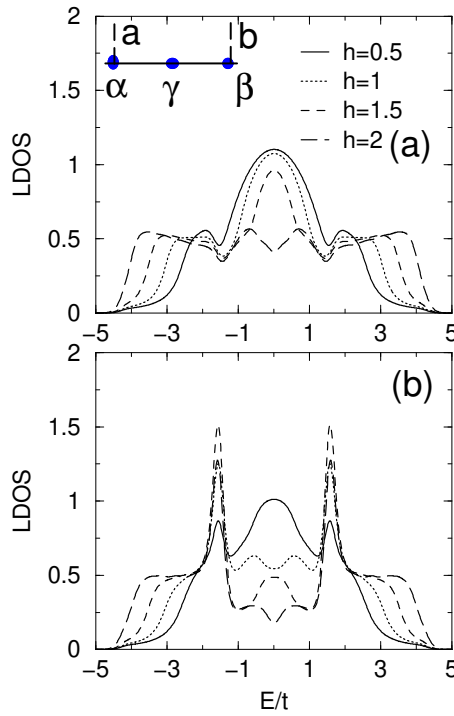


FIG. 8. The LDOS as a function of E/t , for different values of the exchange field, for site a in the interface of a multiterminal junction made of two one-dimensional ferromagnetic electrodes that are connected on top of a two dimensional superconducting system. Sites α, β, γ shown in the inset are in the superconductor while a, b are in the ferromagnetic electrodes. (a) and (b) correspond respectively to the antiparallel and parallel alignment of the magnetization in the ferromagnetic electrodes. The subgap LDOS is larger in the antiferromagnetic alignment.

$$G_{\alpha,\alpha}^{1,2,\text{Ferro}} = -i\pi\rho_0^S \frac{\Delta}{\omega} - i\pi\rho_0^S \frac{\Delta}{\omega} [-f(x_a) - f(x_b) - f(x_{c,\uparrow}) - f(x_{c,\downarrow}) + 2f(x_a)f(x_b) + 2f(x_a)f(x_{c,\uparrow}) + 2f(x_b)f(x_{c,\uparrow}) + f(x_a)f(x_{c,\downarrow}) + f(x_b)f(x_{c,\downarrow}) + f(x_{c,\uparrow})f(x_{c,\downarrow})] \quad (23)$$

$$G_{\alpha,\alpha}^{1,2,\text{Antiferro}} = -i\pi\rho_0^S \frac{\Delta}{\omega} - i\pi\rho_0^S \frac{\Delta}{\omega} [-f(x_a) - f(x_b) - f(x_{c,\uparrow}) - f(x_{c,\downarrow}) + 2f(x_a)f(x_{c,\uparrow}) + 2f(x_b)f(x_{c,\downarrow}) + f(x_a)f(x_b) + f(x_a)f(x_{c,\downarrow}) + f(x_b)f(x_{c,\uparrow}) + f(x_{c,\uparrow})f(x_{c,\downarrow})], \quad (24)$$

from what we deduce that the difference between the ferromagnetic and antiferromagnetic superconducting order parameters changes sign if $f(x_{c,\downarrow}) = f(x_a) + f(x_{c,\uparrow})$, in agreement with Fig. 11.

C. Single site Green's functions

The presence or absence of sign changes in $\Delta_{\alpha,\alpha}^F - \Delta_{\alpha,\alpha}^{AF}$ discussed in section VB can also be obtained in the framework of single site Green's functions [6]. In this model the superconducting order parameter is given by

$$\Delta = D \exp \left[-\frac{1}{U\rho_N} (1 + \pi\rho_N\Gamma_\uparrow) (1 + \pi\rho_N\Gamma_\downarrow) \right],$$

where ρ_N is the density of states in the normal state, and where Γ_σ is the total spectral line-width of spin- σ electrons, obtained as the sum of the spectral line-widths associated to each electrode [6]:

$$\Gamma_\sigma = \sum_k |t_{S,\alpha_k}|^2 \rho_{k,\sigma},$$

where t_{S,α_k} is the tunnel amplitude connecting the superconductor and the ferromagnetic electrode α_k .

Electrodes a and b are supposed to have the same spin polarization. We denote by $\gamma = |t_{S,a}|^2 \rho_{a,\uparrow}$ the spectral line-width associated to majority-spin electrons in electrode a and by $\lambda\gamma = |t_{S,a}|^2 \rho_{a,\downarrow}$ the spectral line-width associated to minority-spin electrons in electrode a . The spin polarization of the ferromagnetic electrodes is $P = (1 - \lambda)/(1 + \lambda)$.

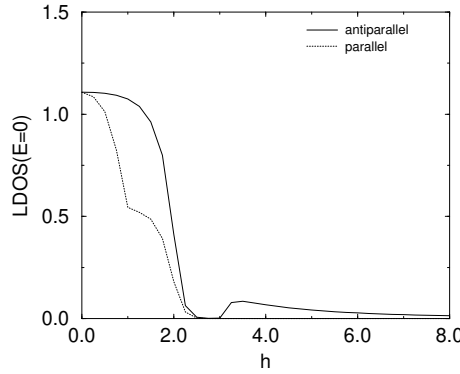


FIG. 9. The local density of states at zero energy at sites a shown in the inset of Fig. 6 as a function of h . The solid line corresponds to antiparallel spin configuration while the dotted line to the parallel spin configuration.

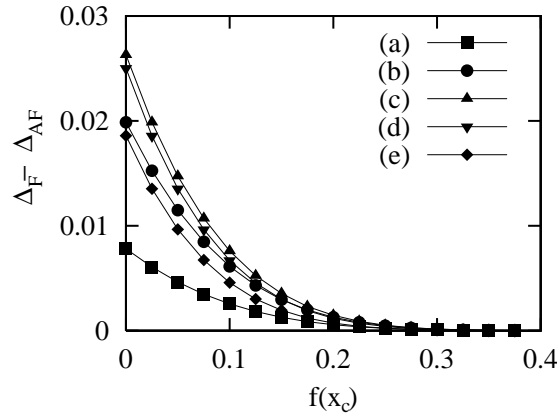


FIG. 10. Variation of $\Delta_{\alpha,\alpha}^F - \Delta_{\alpha,\alpha}^{AF}$ as a function of the transparency of the contact with the normal electrode $f(x_{c,\uparrow}) = f(x_{c,\downarrow})$ for different values of the transparency of the contacts with the ferromagnets $f(x_a) = f(x_b)$. The different curves correspond to (a) $f(x_a) = f(x_b) = 0.05$, (b) $f(x_a) = f(x_b) = 0.1$, (c) $f(x_a) = f(x_b) = 0.15$, (d) $f(x_a) = f(x_b) = 0.2$, (e) $f(x_a) = f(x_b) = 0.25$. We obtain $\Delta_F > \Delta_{AF}$. The microscopic interaction U is such that the superconducting order parameter of the isolated superconductor is $\Delta_{\text{bulk}} = 1$ and the bandwidth of the superconductor is $D = 100$.

We first suppose that electrode c is a ferromagnet having a spin-down orientation with a spectral line-width γ_0 associated to majority-spin electrons and a spectral line-width $\lambda\gamma_0$ associated to minority-spin electrons. If the ferromagnets a and b have a parallel spin orientation the total spectral line-widths are given by $\Gamma_{\uparrow} = 2\gamma + \lambda\gamma_0$ and $\Gamma_{\downarrow} = 2\lambda\gamma + \gamma_0$. If the ferromagnets a and b have an antiparallel spin orientation the total spectral line-widths are given by $\Gamma_{\uparrow} = (1 + \lambda)\gamma + \lambda\gamma_0$ and $\Gamma_{\downarrow} = (1 + \lambda)\gamma + \gamma_0$. We obtain

$$\frac{\Delta_F}{\Delta_{AF}} = \exp \left[\frac{\pi^2 \rho_N}{U} (1 - \lambda)^2 (\gamma^2 - \gamma_0^2) \right],$$

from what we deduce that $\Delta_F > \Delta_{AF}$ if $\gamma_0 < \gamma$ and $\Delta_F < \Delta_{AF}$ if $\gamma_0 > \gamma$, in agreement with the microscopic model discussed in section V B. A similar calculation in the case where electrode c is a spin-up ferromagnet shows that there is no sign change in $\Delta_F - \Delta_{AF}$.

We suppose now that electrode c is a normal metal with a spectral line-width γ_0 associated to spin-up and spin-down electrons. We obtain

$$\frac{\Delta_F}{\Delta_{AF}} = \exp \left[\frac{\pi^2 \rho_N}{U} (1 - \lambda)^2 \gamma^2 \right]$$

which leads to $\Delta_F > \Delta_{AF}$ for all values of γ_0 , in agreement with section V B.

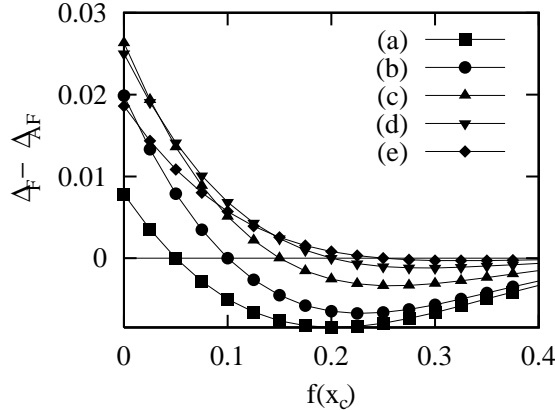


FIG. 11. Variation of $\Delta_{\alpha,\alpha}^F - \Delta_{\alpha,\alpha}^{AF}$ as a function of the transparency of the contact with the spin-down ferromagnetic electrode $f(x_{c,\downarrow})$ ($f(x_{c,\uparrow}) = 0$) for different values of the transparency of the contacts with the ferromagnets $f(x_a) = f(x_b)$. The different curves correspond to (a) $f(x_a) = f(x_b) = 0.05$, (b) $f(x_a) = f(x_b) = 0.1$, (c) $f(x_a) = f(x_b) = 0.15$, (d) $f(x_a) = f(x_b) = 0.2$, (e) $f(x_a) = f(x_b) = 0.25$. $\Delta_F - \Delta_{AF}$ changes sign as the transparency of the contact with electrode c increases. The microscopic interaction U is such that the superconducting order parameter of the isolated superconductor is $\Delta_{\text{bulk}} = 1$ and the bandwidth of the superconductor is $D = 100$.

D. Diagonalizations of the Bogoliubov-de Gennes Hamiltonian

We consider exact diagonalizations of the Bogoliubov-de Gennes Hamiltonian in a situation where a two-dimensional superconducting system is connected to two one-dimensional ferromagnetic electrodes and to a one-dimensional normal metal electrode. We show that the proximity effect in the normal metal electrode can be controlled by the spin orientation of the two ferromagnetic electrodes in the sense that the LDOS in the normal metal electrode depends strongly on the relative spin orientation of the ferromagnetic electrodes. The LDOS at points a and c are shown on Figs. 12(a) and 12(b). It is visible on Fig. 12(b) that the zero-energy LDOS decreases strongly with increasing the exchange field in the ferromagnetic alignment while it is almost independent on the exchange field in the anti-ferromagnetic alignment. This can be understood by assuming that the main contribution to the LDOS is due to crossed Andreev reflections [4]. In the ferromagnetic alignment spin-up electrons in electrodes a and b are coupled to spin-down holes in electrode c . In the antiferromagnetic alignment spin-up electrons in electrode a are coupled to spin-down holes in electrode c while spin-down electrons in electrode b are coupled to spin-up holes in electrode c . Therefore in the calculation of the LDOS given by (19) only one spin polarization contributes in the case of the ferromagnetic alignment while the two spin polarizations contribute in the case the antiferromagnetic alignment. This explains qualitatively why the LDOS is larger in the antiferromagnetic alignment.

The variation of the pair amplitude as a function of the transparency t_c of the normal metal electrode is shown on Fig. 13. For a small t_c the pair amplitude is larger in the ferromagnetic alignment, which is in agreement with the analytical calculations presented in sections IV A, IV B and V A. The difference changes sign as t_c increases. We note that this change of sign occurs for artificially large values of t_c but it is not predicted by the analytical model analyzed in section V A. This is likely to be due to the fact that the analytical calculation is based on the evaluation of the Gorkov function at high energy while low energy degrees of freedom play a role in the the numerical simulation.

VI. TRANSPORT PROPERTIES

In this section we consider transport properties across one of the electrodes connected to the superconductor (see Figs. 1, 14).

A. Transport through a ferromagnetic electrode in the vicinity of another ferromagnetic electrode

We first consider the situation on Fig. 14 in which a ferromagnetic point contact (electrode a) is connected to a superconductor in the vicinity of another ferromagnetic electrode (electrode b). A voltage V is applied on electrode

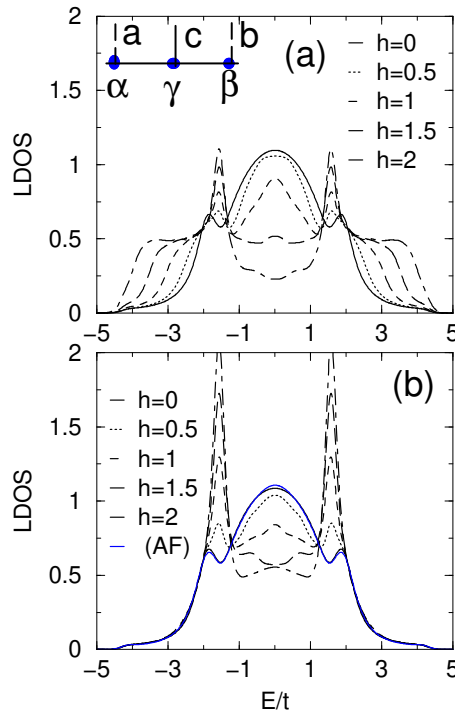


FIG. 12. (a) The LDOS as a function of E/t for site a in the interface of a multiterminal junction made of two one-dimensional ferromagnetic electrodes and one one-dimensional normal metal electrode that are connected on top of a two dimensional superconducting system, for the parallel alignment of spins in the ferromagnetic electrodes. (b) The same as (a) but for site c . The curve labeled as AF corresponds to the antiferromagnetic alignment of the magnetic moments in the ferromagnetic electrodes for $h = 2$.

a and no voltage is applied on electrode b . There is thus no current flow through electrode b . We first suppose in section VIA 1 that the two ferromagnetic electrodes are half-metal ferromagnets. It was shown in Ref. [7] in the context of crossed Andreev reflections that extended contacts can be well described by averaging out the electronic phase if the distance between the ferromagnetic electrodes is large compared to the Fermi wave-length. In the models considered here, the average over the phase variables $\varphi_{\alpha,\beta}$ (see Eqs. 7 and 8) can be carried out analytically and we obtain an expansion of the average current as a series in $t_{a,\alpha}$ and $t_{b,\beta}$. The case of a partial spin polarization is treated in section VIA 2.

1. Half-metal ferromagnets

Since we suppose that a voltage V is applied on electrode a only (see Fig. 14) the current is obtained by evaluating the Keldysh Green's function in a perturbation in $t_{a,\alpha}$. The final expression of the current is non perturbative since we re-sum the perturbative series to all orders. The first step is to evaluate the Green's function \hat{G} of the system in which electrodes a and b are connected to the superconductor in terms of the Green's function \hat{g} of the system in which electrode a is disconnected while electrode b is connected. The second step is to relate the Green's function \hat{g} to the Green's function \hat{g}_0 of the system where electrodes a and b are disconnected.

We consider in this section the situation where the two ferromagnetic electrodes are half-metal ferromagnets. There is thus no subgap transport. The transport formula is found to be [40,41]

$$I = \int \frac{4\pi^2 t_{a,\alpha}^2 \rho_a \rho_{g,1,1}^{\alpha,\alpha}}{\left(1 + \pi^2 t_{a,\alpha}^2 \rho_a \rho_{g,1,1}^{\alpha,\alpha}\right)^2} [n_F(\omega - eV_a) - n_F(\omega - eV_S)]. \quad (25)$$

The local density of state $\rho_{g,1,1}^{\alpha,\alpha}$ at site α contains a “local” term $\rho_{g,0}$ plus a contribution due to the excursions of the electrons in electrode b :

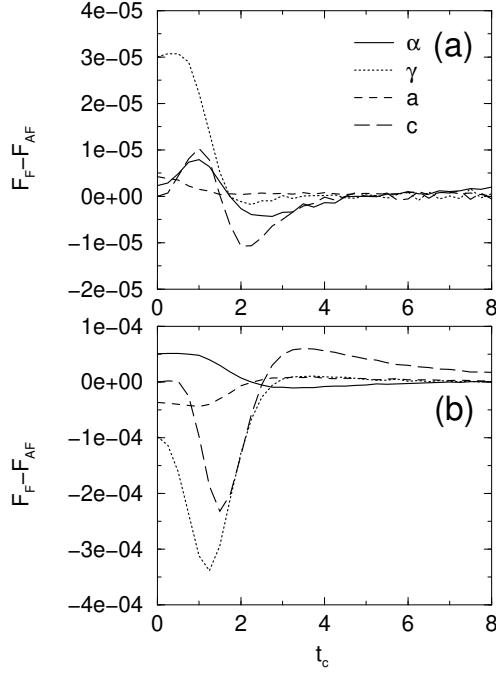


FIG. 13. (a) The difference in the pair amplitude (F) for the ferromagnetic and the antiferromagnetic alignment of the magnetic moments in the ferromagnetic electrodes at the sites α, γ, a, c shown in the insert of Fig. 8, for $t_a = 1t$, as a function of t_c . (b) The same as in (a) but for $t_a = 5t$.

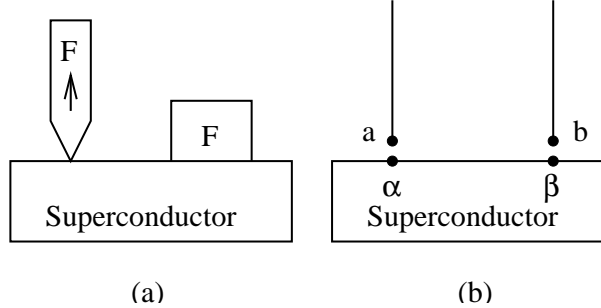


FIG. 14. (a) Schematic representation of the point contact experiment involving two ferromagnetic electrodes. (b) The notation used in the model. The superconducting order parameter at point α depends on the relative spin orientation of the two ferromagnetic electrodes. This can be detected by measuring the voltage dependence of the current through electrode a .

$$\rho_{g,1,1}^{\alpha,\alpha,F} = \rho_{g,0} - \frac{\pi^2 t_{b,\beta}^2 \rho_b}{1 + \pi^2 t_{b,\beta}^2 \rho_{g,0} \rho_b} \text{Re} \left[\rho_{g,0}^{\alpha,\beta} \rho_{g,0}^{\beta,\alpha} \right] \quad (26)$$

$$\rho_{g,1,1}^{\alpha,\alpha,AF} = \rho_{g,0} - \frac{\pi^2 t_{b,\beta}^2 \rho_b}{1 + \pi^2 t_{b,\beta}^2 \rho_{g,0} \rho_b} \text{Re} \left[\rho_{f,0}^{\alpha,\beta} \rho_{f,0}^{\beta,\alpha} \right], \quad (27)$$

where the ordinary and anomalous density of state $\rho_{g,0}$ and $\rho_{f,0}$ are given in Eqs. (9 and (10)). To obtain the current we average the density of states over the microscopic phase variables and inject the average density of states in the transport formula given by (25). We use the following identity:

$$\langle \langle \text{Re} \left[\left(\rho_{g,0}^{\alpha,\beta} \right)^2 \right] \rangle \rangle = \langle \langle \text{Re} \left[\left(\rho_{f,0}^{\alpha,\beta} \right)^2 \right] \rangle \rangle = \frac{1}{2} \left(\rho_0^S \right)^2 \left(\frac{a_0}{R_{\alpha,\beta}} \right)^2 \frac{\Delta_{\alpha,\beta}^2}{\omega^2 - \Delta_{\alpha,\beta}^2}. \quad (28)$$

In the context of crossed Andreev reflection this identity ensures that to lowest order the average elastic cotunneling conductance is equal to the average Andreev reflection conductance [5]. In the context of the point contact experiment on Fig. 14 the identity (28) ensures that the average density of state at site α is independent on the spin orientation

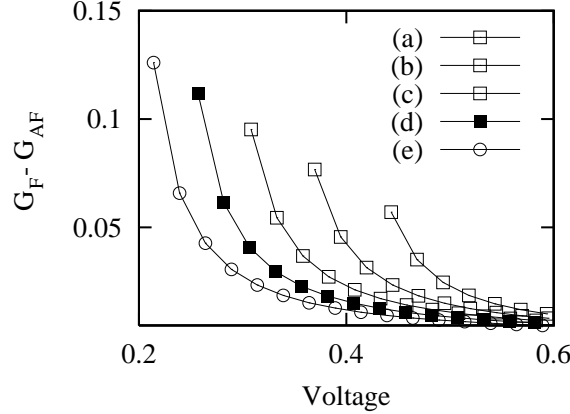


FIG. 15. Voltage dependence of the difference between the conductances in the ferromagnetic and antiferromagnetic alignments for two half-metal ferromagnets connected to the same site in the superconductor. We used the parameters $t_{a,\alpha} = t_{b,\beta} = 1$, $\rho_0^S = 1$. The values of the density of state are the following: (a) $\rho_a = 0.01$; (b) $\rho_a = 0.012$; (c) $\rho_a = 0.014$; (d) $\rho_a = 0.016$; (e) $\rho_a = 0.018$. The values of ρ_b are such that $\rho_b = \rho_a$. The quasiparticle current is such that $G_F > G_{AF}$ in a situation where $\Delta^F > \Delta^{AF}$. The microscopic interaction U is such that the bulk superconducting gap is $\Delta_{\text{bulk}} = 1$ and the bandwidth of the superconductor is $D = 100$.

of electrode b :

$$\langle\langle \rho_{g,1,1}^{\alpha,\alpha,F} \rangle\rangle = \langle\langle \rho_{g,1,1}^{\alpha,\alpha,AF} \rangle\rangle = \rho_{g,0} - \frac{1}{2} \frac{\pi^2 t_{b,\beta}^2 \rho_b}{1 + \pi^2 t_{b,\beta}^2 \rho_{g,0} \rho_b} (\rho_0^S)^2 \left(\frac{a_0}{R_{\alpha,\beta}} \right)^2 \frac{\Delta_{\alpha,\beta}^2}{\omega^2 - \Delta_{\alpha,\beta}^2}.$$

To evaluate the difference $G_F - G_{AF}$ between the conductances in the ferromagnetic and antiferromagnetic alignments we suppose that the distance between the electrodes is smaller than the superconducting coherence length but much larger than the Fermi wavelength. With this assumption the superconducting order parameter can be evaluated within a “local” model in which the two electrodes are connected to the same site. Because the distance between the ferromagnetic electrodes is larger than the Fermi wave-length we average out the electronic phases in the local density of states. As shown on Fig. 15 the conductance associated to quasiparticle transport is larger in the ferromagnetic alignment than in the antiferromagnetic alignment ($G_F > G_{AF}$).

2. Partial spin polarization

a. Andreev reflection current Now we consider the situation where electrodes a and b have a partial spin polarization. The spin-up Andreev reflection current is found to be [40]

$$I_{\uparrow}^{\text{AR}} = \int \frac{4\pi^2 t_{a,\alpha}^4 \rho_{a,\uparrow} \rho_{a,\downarrow}}{|\mathcal{D}|^2} |f_{\alpha,\alpha}|^2 [n_F(\omega + eV_a) - n_F(\omega - eV_a)] d\omega,$$

with

$$\mathcal{D} = 1 - i\pi t_{a,\alpha}^2 (\rho_{a,\uparrow} + \rho_{a,\downarrow}) g_{\alpha,\alpha} + \pi^2 t_{a,\alpha}^4 \rho_{a,\uparrow} \rho_{a,\downarrow} (f_{\alpha,\alpha}^2 - g_{\alpha,\alpha}^2).$$

The propagators $g_{\alpha,\alpha}$ and $f_{\alpha,\alpha}$ are given by

$$g_{\alpha,\alpha}^{1,1} = g_0 + \frac{i\pi t_{b,\beta}^2}{\mathcal{D}'} \left\{ g_{0,\alpha,\beta} \rho_{b,\uparrow} [g_{0,\beta,\alpha} + i\pi t_{b,\beta}^2 \rho_{b,\downarrow} (f_0 f_{0,\beta,\alpha} - g_0 g_{0,\beta,\alpha})] \right. \quad (29)$$

$$\left. + f_{0,\alpha,\beta} \rho_{b,\downarrow} [f_{0,\beta,\alpha} + i\pi t_{b,\beta}^2 \rho_{b,\uparrow} (f_0 g_{0,\beta,\alpha} - g_0 f_{0,\beta,\alpha})] \right\}$$

$$g_{\alpha,\alpha}^{2,2} = g_0 + \frac{i\pi t_{b,\beta}^2}{\mathcal{D}'} \left\{ f_{0,\alpha,\beta} \rho_{b,\uparrow} [f_{0,\beta,\alpha} + i\pi t_{b,\beta}^2 \rho_{b,\downarrow} (f_0 g_{0,\beta,\alpha} - g_0 f_{0,\beta,\alpha})] \right. \quad (30)$$

$$\left. + g_{0,\alpha,\beta} \rho_{b,\downarrow} [g_{0,\beta,\alpha} + i\pi t_{b,\beta}^2 \rho_{b,\uparrow} (f_0 f_{0,\beta,\alpha} - g_0 g_{0,\beta,\alpha})] \right\}$$

$$f_{\alpha,\alpha} = f_0 + \frac{i\pi t_{b,\beta}^2}{\mathcal{D}'} \left\{ g_{0,\alpha,\beta} \rho_{b,\uparrow} [f_{0,\beta,\alpha} + i\pi t_{b,\beta}^2 \rho_{b,\downarrow} (f_0 g_{0,\beta,\alpha} - g_0 f_{0,\beta,\alpha})] \right. \quad (31)$$

$$\left. + f_{0,\alpha,\beta} \rho_{b,\downarrow} [g_{0,\beta,\alpha} + i\pi t_{b,\beta}^2 \rho_{b,\uparrow} (f_0 f_{0,\beta,\alpha} - g_0 g_{0,\beta,\alpha})] \right\},$$

with

$$\mathcal{D}' = 1 - i\pi t_{b,\beta}^2(\rho_{b,\uparrow} + \rho_{b,\downarrow})g_0 + \pi^2 t_{b,\beta}^4(f_0^2 - g_0^2)\rho_{b,\uparrow}\rho_{b,\downarrow}.$$

We use the identity (28) to average over disorder and we obtain

$$\langle\langle g_{\alpha,\alpha}^{1,1} \rangle\rangle = \langle\langle g_{\alpha,\alpha}^{2,2} \rangle\rangle = g_0 + \frac{i\pi^3 t_{b,\beta}^2 (\rho_0^S)^2 (\rho_{b,\uparrow} + \rho_{b,\downarrow})}{2\mathcal{D}'} \left(\frac{a_0}{R_{\alpha,\beta}} \right)^2 \frac{\Delta^2}{\Delta^2 - \omega^2} \exp \left[-\frac{R_{\alpha,\beta}}{\xi(\omega)} \right] \quad (32)$$

$$\langle\langle g_{\alpha,\alpha}^{1,2} \rangle\rangle = f_0 + \frac{i\pi t_{b,\beta}^2}{2\mathcal{D}'} (\pi\rho_0^S)^2 \left(\frac{a_0}{R_{\alpha,\beta}} \right)^2 \exp \left[-\frac{R_{\alpha,\beta}}{\xi(\omega)} \right] \frac{\Delta}{\sqrt{\Delta^2 - \omega^2}} \left\{ (\rho_{b,\uparrow} + \rho_{b,\downarrow}) \frac{-\omega}{\sqrt{\Delta^2 - \omega^2}} + 2i\pi t_{b,\beta}^2 \rho_{b,\uparrow} \rho_{b,\downarrow} \rho_0^S \right\}. \quad (33)$$

As a result the form of the transport formula is identical in the two spin orientations of electrode b . Still the current depends on the spin orientation of electrode b because the self-consistent superconducting order parameter depends on the spin orientation of electrode b .

b. *Quasiparticle current* The spin-up quasiparticle current takes the form

$$I_{\uparrow}^{\text{qp}} = \int \frac{4\pi^2 t_{a,\alpha}^2 \rho_{a,\uparrow}}{\mathcal{D}^2} \left\{ \rho_g^{\alpha,\alpha} \left[1 + 2\pi^2 t_{a,\alpha}^2 \rho_{a,\downarrow} \rho_g^{\alpha,\alpha} + \pi^4 t_{a,\alpha}^4 (\rho_{a,\downarrow}^2 (\rho_g^{\alpha,\alpha})^2 + \rho_{a,\uparrow}^2 (\rho_f^{\alpha,\alpha})^2 - 2\rho_{a,\downarrow}^2 (\rho_f^{\alpha,\alpha})^2) \right] \right. \\ \left. - 2\pi^2 t_{a,\alpha}^2 \rho_{a,\downarrow} (\rho_f^{\alpha,\alpha})^2 \right\}, \quad (34)$$

with

$$\mathcal{D} = 1 + \pi^2 t_{a,\alpha}^2 (\rho_{a,\uparrow} + \rho_{a,\downarrow}) \rho_g^{\alpha,\alpha} + \pi^4 t_{a,\alpha}^4 \rho_{a,\uparrow} \rho_{a,\downarrow} ((\rho_g^{\alpha,\alpha})^2 - (\rho_f^{\alpha,\alpha})^2).$$

The density of states $\rho_g^{\alpha,\alpha}$ and $\rho_f^{\alpha,\alpha}$ are given by $\rho_g^{\alpha,\alpha} = \frac{1}{\pi} \text{Im}[g_{\alpha,\alpha}^{1,1}]$ and $\rho_f^{\alpha,\alpha} = \frac{1}{\pi} \text{Im}[g_{\alpha,\alpha}^{1,2}]$, with

$$g_{\alpha,\alpha}^{1,1} = i\pi \rho_{g,0} - \frac{i\pi^3 t_{b,\beta}^2}{\mathcal{D}'} \left\{ \rho_{g,0}^{\alpha,\beta} \rho_{b,\uparrow} \left[\rho_{g,0}^{\beta,\alpha} + \pi^2 t_{b,\beta}^2 \rho_{b,\downarrow} \left(\rho_{g,0} \rho_{g,0}^{\beta,\alpha} - \rho_{f,0} \rho_{f,0}^{\beta,\alpha} \right) \right] \right. \\ \left. + \rho_{f,0}^{\alpha,\beta} \rho_{b,\downarrow} \left[\rho_{f,0}^{\beta,\alpha} + \pi^2 t_{b,\beta}^2 \rho_{b,\uparrow} \left(\rho_{g,0} \rho_{f,0}^{\beta,\alpha} - \rho_{f,0} \rho_{g,0}^{\beta,\alpha} \right) \right] \right\} \quad (35)$$

$$g_{\alpha,\alpha}^{1,2} = i\pi \rho_{f,0} - \frac{i\pi^3 t_{b,\beta}^2}{\mathcal{D}'} \left\{ \rho_{g,0}^{\alpha,\beta} \rho_{b,\uparrow} \left[\rho_{f,0}^{\beta,\alpha} + \pi^2 t_{b,\beta}^2 \rho_{b,\downarrow} \left(\rho_{g,0} \rho_{f,0}^{\beta,\alpha} - \rho_{f,0} \rho_{g,0}^{\beta,\alpha} \right) \right] \right. \\ \left. + \rho_{f,0}^{\alpha,\beta} \rho_{b,\downarrow} \left[\rho_{g,0}^{\beta,\alpha} + \pi^2 t_{b,\beta}^2 \rho_{b,\uparrow} \left(\rho_{g,0} \rho_{g,0}^{\beta,\alpha} - \rho_{f,0} \rho_{f,0}^{\beta,\alpha} \right) \right] \right\}, \quad (36)$$

and with

$$\mathcal{D}' = 1 + \pi^2 t_{b,\beta}^2 (\rho_{b,\uparrow} + \rho_{b,\downarrow}) \rho_{g,0} + \pi^4 t_{b,\beta}^4 (\rho_{g,0}^2 - \rho_{f,0}^2) \rho_{b,\uparrow} \rho_{b,\downarrow}.$$

The average density of states is given by

$$\frac{1}{\pi} \text{Im} \langle\langle g_{\alpha,\alpha}^{1,1} \rangle\rangle = \frac{1}{\pi} \text{Im} \langle\langle g_{\alpha,\alpha}^{2,2} \rangle\rangle = \rho_{g,0} - \frac{1}{2} \frac{\pi^2 t_{b,\beta}^2}{\mathcal{D}'} (\rho_0^S)^2 \left(\frac{a_0}{R_{\alpha,\beta}} \right)^2 \frac{\Delta^2}{\omega^2 - \Delta^2} (\rho_{b,\uparrow} + \rho_{b,\downarrow}),$$

which depends on the spin orientation of electrode b through the fact that the superconducting order parameter depends on the spin orientation of electrode b .

The voltage dependence of the average current for partially spin polarized ferromagnets is shown on Fig. 16. The transition from Andreev reflection to quasiparticle transport occurs at a voltage $V_{\text{AF}} = \Delta_{\text{AF}}$ in the antiferromagnetic spin orientation, smaller than the voltage $V_{\text{F}} = \Delta_{\text{F}}$ in the ferromagnetic spin orientation. As a result we obtain $G_{\text{F}} - G_{\text{AF}} < 0$ if $V < \Delta_{\text{F}}$ and $G_{\text{F}} - G_{\text{AF}} > 0$ if $V > \Delta_{\text{F}}$.

B. Transport through a ferromagnetic electrode in the vicinity of two other ferromagnetic electrodes

We consider in this section the point contact experiment on Fig. 1 in which electrode c is a half-metal ferromagnetic channel with a spin-down orientation. The transport formula was already given in section VI A 1. In the situation where electrodes a and b have a spin-up orientation the Green's function $g_{2,2}^{\gamma,\gamma}$ at point γ is given by

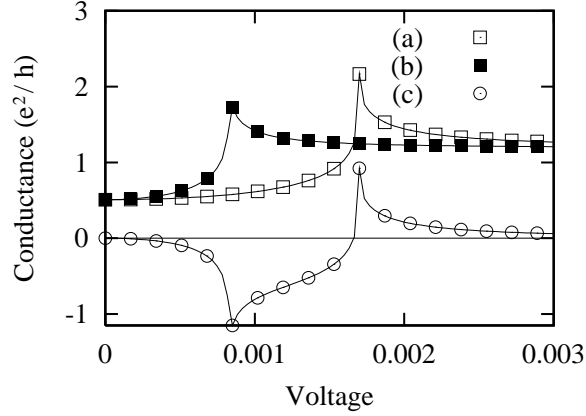


FIG. 16. Variation of the average Andreev reflection and quasiparticle current with partially polarized ferromagnets in the point contact experiment shown on Fig. 14. We have shown the voltage dependence of the conductance in the ferromagnetic alignment of the spin orientation of the two electrodes (□) in the antiferromagnetic alignment (■) and the difference $G_F - G_{AF}$ between the conductances in the ferromagnetic and antiferromagnetic spin orientations (○). We used the parameters $\rho_0^S = 1$, $t_{a,\alpha}^2 = t_{b,\beta}^2 = 1$, $\rho_{a,\uparrow} = 0.05$ and $\rho_{a,\downarrow} = 0.01$. In the ferromagnetic alignment we have $\rho_{b,\uparrow} = \rho_{a,\uparrow}$ and $\rho_{b,\downarrow} = \rho_{a,\downarrow}$. In the antiferromagnetic alignment we have $\rho_{b,\uparrow} = \rho_{a,\downarrow}$ and $\rho_{b,\downarrow} = \rho_{a,\uparrow}$. The microscopic interaction U is such that the bulk superconducting gap is $\Delta_{bulk} = 1$ and the bandwidth of the superconductor is $D = 100$. We obtain a qualitatively similar behavior in the case of the point contact experiment on Fig. 1.

$$g_{\gamma,\gamma}^{2,2} = i\pi \left\{ \rho_{g,0} - \frac{\pi^2 t_{a,\alpha}^2 \rho_a [1 + \pi^2 t_{b,\beta}^2 \rho_b \rho_{g,0}]}{\mathcal{D}_{b,\uparrow}} \rho_{f,0}^{\alpha,\gamma} \rho_{f,0}^{\gamma,\alpha} + \frac{\pi^4 t_{a,\alpha}^2 t_{b,\beta}^2 \rho_a \rho_b}{\mathcal{D}_{b,\uparrow}} \rho_{f,0}^{\gamma,\alpha} \rho_{g,0}^{\alpha,\beta} \rho_{f,0}^{\beta,\gamma} \right. \\ \left. + \frac{\pi^4 t_{a,\alpha}^2 t_{b,\beta}^2 \rho_a \rho_b}{\mathcal{D}_{b,\uparrow}} \rho_{f,0}^{\gamma,\beta} \rho_{g,0}^{\beta,\alpha} \rho_{f,0}^{\alpha,\gamma} - \frac{\pi^2 t_{b,\beta}^2 \rho_b [1 + \pi^2 t_{a,\alpha}^2 \rho_a \rho_{g,0}]}{\mathcal{D}_{b,\uparrow}} \rho_{f,0}^{\gamma,\beta} \rho_{f,0}^{\beta,\gamma} \right\}, \quad (37)$$

with

$$\mathcal{D}_{b,\uparrow} = [1 + \pi^2 t_{a,\alpha}^2 \rho_a \rho_{g,0}] [1 + \pi^2 t_{b,\beta}^2 \rho_b \rho_{g,0}] - \pi^4 t_{a,\alpha}^2 t_{b,\beta}^2 \rho_a \rho_b \rho_{g,0}^{\alpha,\beta} \rho_{g,0}^{\beta,\alpha}$$

In the situation where electrode a has a spin-up orientation and electrodes b and c have a spin-down orientation the Green's function $g_{2,2}^{\gamma,\gamma}$ at point γ is given by

$$g_{\gamma,\gamma}^{2,2} = i\pi \left\{ \rho_{g,0} - \frac{\pi^2 t_{a,\alpha}^2 \rho_a [1 + \pi^2 t_{b,\beta}^2 \rho_b \rho_{g,0}]}{\mathcal{D}_{b,\downarrow}} \rho_{f,0}^{\alpha,\gamma} \rho_{f,0}^{\gamma,\alpha} + \frac{\pi^4 t_{a,\alpha}^2 t_{b,\beta}^2 \rho_a \rho_b}{\mathcal{D}_{b,\downarrow}} \rho_{f,0}^{\gamma,\alpha} \rho_{f,0}^{\alpha,\beta} \rho_{f,0}^{\beta,\gamma} \right. \\ \left. + \frac{\pi^4 t_{a,\alpha}^2 t_{b,\beta}^2 \rho_a \rho_b}{\mathcal{D}_{b,\downarrow}} \rho_{g,0}^{\gamma,\beta} \rho_{f,0}^{\beta,\alpha} \rho_{f,0}^{\alpha,\gamma} - \frac{\pi^2 t_{b,\beta}^2 \rho_b [1 + \pi^2 t_{a,\alpha}^2 \rho_a \rho_{g,0}]}{\mathcal{D}_{b,\downarrow}} \rho_{g,0}^{\gamma,\beta} \rho_{g,0}^{\beta,\gamma} \right\}, \quad (38)$$

with

$$\mathcal{D}_{b,\downarrow} = [1 + \pi^2 t_{a,\alpha}^2 \rho_a \rho_{g,0}] [1 + \pi^2 t_{b,\beta}^2 \rho_b \rho_{g,0}] - \pi^4 t_{a,\alpha}^2 t_{b,\beta}^2 \rho_a \rho_b \rho_{f,0}^{\alpha,\beta} \rho_{f,0}^{\beta,\alpha}.$$

Using the identities

$$\langle\langle (\rho_{g,0}^{\alpha,\beta})^{2n} \rangle\rangle = \langle\langle (\rho_{f,0}^{\alpha,\beta})^{2n} \rangle\rangle = \binom{2n}{n} \left(\frac{\rho_{f,0}}{2R_{\alpha,\beta}} \right)^{2n}$$

that generalize Eq. (28), we obtain the density of states at point γ :

$$\frac{1}{\pi} \text{Im} g_{\gamma,\gamma}^{2,2} = \rho_{g,0} - 2\rho_{f,0} \left[X_a \left(\frac{a_0}{2R_{\alpha,\gamma}} \right)^2 + X_b \left(\frac{a_0}{2R_{\beta,\gamma}} \right)^2 \right] \sum_{n=0}^{+\infty} \binom{2n}{n} \left[\left(\frac{a_0}{2R_{\alpha,\beta}} \right)^2 X_a X_b \right]^n,$$

with

$$X_{a,b} = \frac{\pi^2 t_{a,\alpha}^2 \rho_{a,b} \rho_{f,0}}{1 + \pi^2 t_{a,\alpha}^2 \rho_{a,b} \rho_{g,0}}.$$

The density of states depends on $\rho_{f,0}$ and $\rho_{g,0}$ that are a function of the superconducting order parameter. The superconducting order parameter is different in the ferromagnetic and antiferromagnetic alignments and this is why the density of states and the current are different in the two spin orientations. The variation of the difference between the conductances in the ferromagnetic and antiferromagnetic alignments as a function of $|t_{c,\gamma}|^2$ is shown on Fig. 17. It is visible that $G_F - G_{AF}$ changes sign for $|t_{c,\gamma}|^2 = 0.05$. At this point the difference between the superconducting order parameters in the ferromagnetic and antiferromagnetic alignments also changes sign. This shows that the change of sign in $\Delta_F - \Delta_{AF}$ can be probed in a point contact experiment.

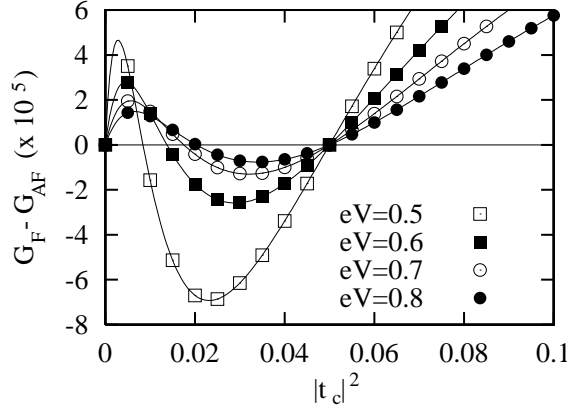


FIG. 17. Variation of $G_F - G_{AF}$ versus $|t_c|^2$ for different values of the bias voltage. The parameters are the following: $\rho_0^S = 1$, $|t_a|^2 = |t_b|^2 = 0.05$, $\rho_a = \rho_b = \rho_c = 0.05$. The difference between the superconducting order parameter in the ferromagnetic and antiferromagnetic alignments changes sign for $|t_c|^2 = 0.05$. At this point the difference between the conductances in the ferromagnetic and antiferromagnetic alignments also changes sign.

VII. CONCLUSION

To conclude we have provided a detailed investigation of multi-connected hybrid structures in which three electrodes are connected to a superconductor. We have first reconsidered FSF heterostructures in which two ferromagnetic electrodes are connected to a superconductor at a distance smaller than the superconducting coherence length. We have found that within a “local” model the superconducting order parameter in the ferromagnetic alignment is larger than the superconducting order parameter in the antiferromagnetic alignment, in agreement with a different model discussed in Ref. [8]. We have shown that the zero-energy LDOS in the antiferromagnetic alignment is larger than the zero-energy LDOS in the ferromagnetic alignment. In the case where two ferromagnetic and a normal metal electrode are connected to a superconductor we have found that the LDOS in the normal metal depends strongly on the spin orientation in the ferromagnetic electrodes. In this respect, the proximity effect in the normal metal can be controlled by the relative spin orientation of the ferromagnetic electrodes. If the normal metal is replaced by a ferromagnetic metal with a spin-down orientation we have found that $\Delta_{AF} > \Delta_F$ for high transparencies and we have provided two analytical models for this behavior (an inversion of the 4×4 Dyson matrix for half-metal ferromagnets and another approach based on effective Green’s functions for partially polarized ferromagnets). This behavior was not confirmed by the exact diagonalizations of the Bogoliubov-de Gennes equations which is likely to be due to the fact that low energy degrees of freedom play a role in the exact diagonalization whereas the analytical approach are based on an evaluation of the Gorkov function at high energy.

We have also calculated transport properties associated to point contact experiments and discussed the role of phase averaging in the ordinary and anomalous propagators. We have established non perturbative transport formula and found that the current depends on the relative spin orientation of the ferromagnetic electrodes because the superconducting order parameter is different in the ferromagnetic and antiferromagnetic alignments. If the voltage is smaller than the superconducting order parameter in the ferromagnetic alignment ($eV < \Delta_F$) we found that

$G_{\text{AF}} > G_{\text{F}}$ whereas $G_{\text{F}} > G_{\text{AF}}$ if $eV > \Delta_{\text{F}}$. This behavior at low voltage is in agreement with the fact that the low energy LDOS is larger in the antiferromagnetic alignment due to crossed Andreev reflections. We have shown that the change of sign in $\Delta_{\text{F}} - \Delta_{\text{AF}}$ obtained with three ferromagnetic electrodes can be probed in a transport experiment.

ACKNOWLEDGEMENT

The authors acknowledge fruitful discussions with D. Feinberg, M. Giroud and H. Courtois.

APPENDIX A: EXPRESSION OF THE LOCAL GORKOV FUNCTIONS FOR TWO FERROMAGNETIC ELECTRODES WITH A PARTIAL SPIN POLARIZATION

We give the expression of the Gorkov functions $G_{\alpha,\alpha}^{1,2}$ and $G_{\beta,\beta}^{1,2}$ for the system on Fig. 2-(b) in which two ferromagnetic electrodes are connected to a superconductor at points α and β . We suppose that the distance between α and β is comparable to the superconducting coherence length.

The inversion of the 4×4 Dyson matrix leads to

$$G_{\alpha,\alpha}^{1,2} = -i\pi\rho_0^S \left\{ \frac{\Delta_{\alpha,\alpha}}{\omega} - \frac{\Delta_{\alpha,\alpha}}{\omega} [f(x_{a,\uparrow}) + f(x_{a,\downarrow}) - f(x_{a,\uparrow})f(x_{a,\downarrow})] \left[1 + (f(x_{a,\uparrow})f(x_{b,\uparrow}) + f(x_{a,\downarrow})f(x_{b,\downarrow})) \left(\frac{a_0}{R_{\alpha,\beta}} \right)^2 \right] - \frac{\Delta_{\alpha,\beta}}{\omega} f(x_{b,\uparrow}) \left(\frac{a_0}{R_{\alpha,\beta}} \right)^2 - \frac{\Delta_{\alpha,\beta}}{\omega} f(x_{b,\downarrow}) \left(\frac{a_0}{R_{\alpha,\beta}} \right)^2 + \left(\frac{\Delta_{\alpha,\alpha}}{\omega} + \frac{\Delta_{\alpha,\beta}}{\omega} \right) f(x_{a,\uparrow})f(x_{b,\uparrow}) \left(\frac{a_0}{R_{\alpha,\beta}} \right)^2 + \left(\frac{\Delta_{\alpha,\alpha}}{\omega} + \frac{\Delta_{\alpha,\beta}}{\omega} \right) f(x_{a,\downarrow})f(x_{b,\downarrow}) \left(\frac{a_0}{R_{\alpha,\beta}} \right)^2 + \frac{\Delta_{\alpha,\beta}}{\omega} f(x_{a,\downarrow})f(x_{b,\uparrow}) \left(\frac{a_0}{R_{\alpha,\beta}} \right)^2 + \frac{\Delta_{\alpha,\beta}}{\omega} f(x_{a,\uparrow})f(x_{b,\downarrow}) \left(\frac{a_0}{R_{\alpha,\beta}} \right)^2 + \frac{\Delta_{\beta,\beta}}{\omega} f(x_{b,\uparrow})f(x_{b,\downarrow}) \left(\frac{a_0}{R_{\alpha,\beta}} \right)^2 - \frac{\Delta_{\alpha,\beta}}{\omega} f(x_{a,\uparrow})f(x_{a,\downarrow})f(x_{b,\uparrow}) \left(\frac{a_0}{R_{\alpha,\beta}} \right)^2 - \frac{\Delta_{\alpha,\beta}}{\omega} f(x_{a,\uparrow})f(x_{a,\downarrow})f(x_{b,\downarrow}) \left(\frac{a_0}{R_{\alpha,\beta}} \right)^2 - \frac{\Delta_{\beta,\beta}}{\omega} f(x_{a,\uparrow})f(x_{b,\uparrow})f(x_{b,\downarrow}) \left(\frac{a_0}{R_{\alpha,\beta}} \right)^2 - \frac{\Delta_{\beta,\beta}}{\omega} f(x_{a,\downarrow})f(x_{b,\uparrow})f(x_{b,\downarrow}) \left(\frac{a_0}{R_{\alpha,\beta}} \right)^2 + \frac{\Delta_{\beta,\beta}}{\omega} f(x_{a,\uparrow})f(x_{a,\downarrow})f(x_{b,\uparrow})f(x_{b,\downarrow}) \left(\frac{a_0}{R_{\alpha,\beta}} \right)^2 \right\} \quad (\text{A1})$$

The expression of $G_{\beta,\beta}^{1,2}$ is obtained by exchanging the sites α and β .

APPENDIX B: EXPRESSION OF THE LOCAL GORKOV FUNCTIONS WITH THREE ELECTRODES AT A DISTANCE SMALLER THAN THE SUPERCONDUCTING COHERENCE LENGTH

1. Ferromagnetic alignment

In the ferromagnetic alignment the inversion of the 4×4 Dyson matrix leads to

$$G_{\alpha,\alpha}^{1,2} = -i\pi\rho_0^S \frac{\Delta}{\omega} - i\pi\rho_0^S \frac{\Delta}{\omega} \frac{1}{\mathcal{D}_{\text{F}}} \left\{ -f(x_a) - f(x_b) - f(x_c,\uparrow) - f(x_c,\downarrow) + 2f(x_a)f(x_b) + 2f(x_a)f(x_c,\uparrow) + 2f(x_b)f(x_c,\uparrow) + f(x_a)f(x_c,\downarrow) + f(x_b)f(x_c,\downarrow) + f(x_c,\uparrow)f(x_c,\downarrow) - 3f(x_a)f(x_b)f(x_c,\uparrow) - f(x_a)f(x_b)f(x_c,\downarrow) - f(x_a)f(x_c,\uparrow)f(x_c,\downarrow) - f(x_b)f(x_c,\uparrow)f(x_c,\downarrow) + f(x_a)f(x_b)f(x_c,\uparrow)f(x_c,\downarrow) \right\}, \quad (\text{B1})$$

with

$$\mathcal{D}_{\text{F}} = 1 - f(x_a)f(x_b) - f(x_a)f(x_c,\uparrow) - f(x_b)f(x_c,\uparrow) + 2f(x_a)f(x_b)f(x_c,\uparrow).$$

2. Antiferromagnetic alignment

In the antiferromagnetic alignment we find

$$G_{\alpha,\alpha}^{1,2} = -i\pi\rho_0^S \frac{\Delta}{\omega} - i\pi\rho_0^S \frac{\Delta}{\omega} \frac{1}{\mathcal{D}_{\text{AF}}} \{ -f(x_a) - f(x_b) - f(x_{c,\uparrow}) - f(x_{c,\downarrow}) + 2f(x_a)f(x_{c,\uparrow}) + 2f(x_b)f(x_{c,\downarrow}) \\ + f(x_a)f(x_b) + f(x_a)f(x_{c,\downarrow}) + f(x_b)f(x_{c,\uparrow}) + f(x_{c,\uparrow})f(x_{c,\downarrow}) - f(x_a)f(x_b)f(x_{c,\downarrow}) \\ - f(x_a)f(x_b)f(x_{c,\uparrow}) - f(x_b)f(x_{c,\uparrow})f(x_{c,\downarrow}) - f(x_a)f(x_{c,\uparrow})f(x_{c,\downarrow}) - f(x_a)f(x_b)f(x_{c,\uparrow})f(x_{c,\downarrow}) \}, \quad (\text{B2})$$

with

$$\mathcal{D}_{\text{AF}} = 1 - f(x_b)f(x_{c,\downarrow}) - f(x_a)f(x_{c,\uparrow}) + f(x_a)f(x_b)f(x_{c,\uparrow})f(x_{c,\downarrow})$$

- [1] M. S. Choi, C. Bruder and D. Loss, Phys. Rev. B **62**, 13569 (2000);
P. Recher, E. V. Sukhorukov and D. Loss, Phys. Rev. B **63**, 165314 (2001).
- [2] D. Feinberg, T. Martin and O. Sauret, cond-mat/0203215.
- [3] G.B. Lesovik, T. Martin, and G. Blatter, arXiv:cond-mat/0009193.
- [4] G. Deutscher and D. Feinberg, App. Phys. Lett. **76**, 487 (2000).
- [5] G. Falci, D. Feinberg, and F.W.J. Hekking, Europhysics Letters **54**, 255 (2001).
- [6] R. Mélin, J. Phys.: Condens. Matter **13**, 6445 (2001);
R. Mélin, to appear in the Proceedings of the XXXVIIth Rencontres de Moriond, T. Martin and G. Montambaux Eds., EDP Sciences (2001).
- [7] R. Mélin and D. Feinberg, Eur. Phys. J. B **26**, 101 (2002).
- [8] V. Apinaryan and R. Mélin, Eur. Phys. J. B **25**, 373 (2002).
- [9] M.J.M. de Jong and C. W. Beenakker, Phys. Rev. Lett. **74**, 1657 (1995).
- [10] R.J. Soulen *et al.*, Science **282**, 85 (1998).
- [11] S.K. Upadhyay *et al.*, Phys. Rev. Lett. **81**, 3247 (1998).
- [12] P. Tedrow and R. Meservey, Phys. Rev. Lett. **26**, 192 (1971);
P. Tedrow and R. Meservey, Phys. Rev. B **7**, 318 (1973);
R. Meservey and P.M. Tedrow, Phys. Rep. **238**, 173 (1994) and references therein.
- [13] P. Fulde and A. Ferrel, Phys. Rev. **135**, A550 (1964).
- [14] A. Larkin and Y. Ovchinnikov, Sov. Phys. JETP **20**, 762 (1965).
- [15] M.A. Clogston, Phys. Rev. Lett. **9**, 266 (1962).
- [16] E.A. Demler, G.B. Arnold and M.R. Beasley, Phys. Rev. B **55**, 15174 (1997).
- [17] A.I. Buzdin, L.N. Bulaevskii, and S.V. Panyukov, JETP Lett. **35**, 178 (1982) [Zh. Eksp. Teor. Fiz. **35**, 147 (1982)].
A. Buzdin, B. Bujicic, and M. Yu. Kupriyanov, Sov. Phys. JETP **74**, 124 (1992) [Zh. Eksp. Teor. Fiz. **101**, 231 (1992)].
- [18] V.V. Ryazanov, V.A. Oboznov, A. Yu. Rusanov, A.V. Veretennikov, A.A. Golubov, J. Aarts, Phys. Rev. Lett. **86**, 2427 (2001).
- [19] T. Kontos, M. Aprili, J. Lesueur, and X. Grison, Phys. Rev. Lett. **86**, 304 (2001).
- [20] A.I. Buzdin and M. Yu. Kupriyanov, JETP Lett. **52**, 487 (1990);
A.I. Buzdin, M. Yu. Kupriyanov and B. Vujicic, Physica C **185 - 189**, 2025 (1991).
- [21] J.S. Jiang, D. Davidović, D.H. Reich, and C.L. Chien, Phys. Rev. Lett. **74**, 314 (1995).
- [22] C.L. Chien, J.S. Jiang, J.Q. Xiao, D. Davidović, and D.H. Reich, J. Appl. Phys. **81**, 5358 (1997).
- [23] L.V. Mercaldo, C. Attanasio, C. Coccores, L. Maritato, S.L. Prischepa, and M. Salvato, Phys. Rev. B **53**, 14 040 (1996).
- [24] J.S. Jiang, D. Davidović, D.H. Reich, and C.L. Chien, Phys. Rev. B **54**, 6119 (1996).
- [25] Th. Muhge, N.N. Garif'yanov, Yu. V. Goryunov, G.G. Khaliullin, L.R. Tagirov, K. Westerholt, I.A. Garifullin, and H. Zabel, Phys. Rev. Lett. **77**, 1857 (1996).
Th. Muhge, K. Westerholt, H. Zabel, N.N. Garif'yanov, Yu. V. Goryunov, I.A. Garifullin, and G.G. Khaliullin, Phys. Rev. B **55**, 8945 (1997).
- [26] M.D. Lawrence and N. Giordano, J. Phys. Condens. Matter **39**, L563 (1996).
- [27] V.A. Vas'ko, V.A. Larkin, P.A. Kraus, K.R. Nikolaev, D.E. Grupp, C.A. Nordman, and A.M. Goldman, Phys. Rev. Lett. **78**, 1134 (1997).
- [28] M. Giroud, H. Courtois, K. Hasselbach, D. Mailly, and B. Pannetier, Phys. Rev. B **58**, R11872 (1998).
- [29] V.T. Petrushov, I.A. Sosnon, I. Cox, A. Parsons, and C. Troadec, Phys. Rev. Lett. **83**, 3281 (1999).

- [30] A.T. Filip, B.H. Hoving, F.J. Jedema, B.J. van Wees, B. Dutta, and S. Borghs, Phys. Rev. B **62**, 9996 (2000).
- [31] M. Giroud, K. Hasselbach, H. Courtois, D. Mailly and B. Pannetier, cond-mat/0204140.
- [32] I. Baladie, A. Buzdin, N. Ryzhanova, and A. Vedyayev, Phys. Rev. B **63**, 054518 (2001).
- [33] P.G. de Gennes, Phys. Letters **23**, 10 (1966).
- [34] G. Deutscher and F. Meunier, Phys. Rev. Lett. **22**, 395 (1969).
- [35] J.J. Hauser, Phys. Rev. Lett. **23**, 374 (1969).
- [36] E. Vecino, A. Martin-Rodero and A. Levy Yeyati, Phys. Rev. B **64**, 184502 (2001).
- [37] P.G. de Gennes, *Superconductivity of Metals and Alloys* (Benjamin, New York, 1966).
- [38] N. Stefanakis, cond-mat/0111250.
- [39] P.G. de Gennes and D. Saint-James, Phys. Lett. **4**, 151 (1963).
- [40] J.C. Cuevas, A. Martin-Rodero, A. Levy Yeyati, Phys. Rev. B **54** 736 (1996).
- [41] Y.A. Genenko and Y.A. Ivanchenko, Theor. Math. Phys. **69**, 1056 (1986).